Smart Health 1–2 (2017) 77–92

Contents lists available at ScienceDirect

Smart Health

journal homepage: www.elsevier.com/locate/smhl

Patient handling activity recognition through pressure-map manifold learning using a footwear sensor

Feng Lin[a], Chen Song[a], Xiaowei Xu[a], Lora Cavuoto[b], Wenyao Xu[a,*]

[a] Department of Computer Science and Engineering, University at Buffalo (SUNY), USA
[b] Department of Industrial and Systems Engineering, University at Buffalo (SUNY), USA

ARTICLE INFO

Keywords:
Patient handling activity
Action manifold learning
Plantar pressure
Smart Insole
Mobile health

ABSTRACT

The risk of overexertion injury caused by patient handling and movement activities causes chronic pain and other physical and social impairments among the nursing force. The accurate recognition of patient handling activities (PHA) is the first step to reduce injury risk for caregivers. The current practice on workplace activity recognition is neither accurate nor convenient to perform. In this paper, we propose a novel solution comprising a smart footwear device and an action manifold learning framework to address the challenge. The wearable device, called Smart Insole, is equipped with a rich set of sensors and can provide an unobtrusive approach to obtain and characterize the action information of patient handling activities. Our proposed action manifold learning (AML) framework extracts the intrinsic signature structure by projecting raw pressure data from a high-dimensional input space to a low-dimensional manifold space. This framework not only performs dimension reduction but also reduces motion artifacts, which is robust against the noise and inter-class/intra-class variation in PHA recognition. To validate the effectiveness of the proposed framework, we perform a pilot study with eight subjects including eight common activities in a nursing room. The intrinsic dimensionality of the manifold is estimated by comparing the residual variances of different dimensionality settings. The experimental results show the overall classification accuracy achieves 86.6%. Meanwhile, the qualitative profile and load level can also be classified with accuracies of 98.9% and 88.3%, respectively.

1. Introduction

All healthcare workers, especially nurses and hospital aids, face a wide range of hazards on the job, such as musculoskeletal disorders related to ergonomic hazards (Public Health Service, 2000). These disorders are associated with excessive back and shoulder loading due to manual patient handling, applying excessive force during pushing and/or pulling of objects, required use of awkward postures during patient care, and working long hours and shiftwork (Waters, Collins, Galinsky, & Caruso, 2006). In 2012 and annually thereafter, overexertion injuries, such as musculoskeletal disorders, low back pain and shoulder pain, accounted for nearly 70 million physician office visits in the United States (Work-related musculoskeletal). The high risk of occupational injuries contributes to severe nurse shortages. The demand for nurses is projected to grow by 22% by 2008, and unless market corrections are made, the nursing shortage may reach 800,000 vacant positions by 2020 (Projected supply, 2002).

The high injury rate of nurses is in part because there is no effective way to monitor the development of chronic injury and detect

* Corresponding author.
E-mail addresses: flin28@buffalo.edu (F. Lin), csong5@buffalo.edu (C. Song), xiaoweix@buffalo.edu (X. Xu), loracavu@buffalo.edu (L. Cavuoto), wenyaoxu@buffalo.edu (W. Xu).

http://dx.doi.org/10.1016/j.smhl.2017.04.005
Received 9 January 2017; Accepted 17 April 2017
Available online 07 May 2017
2352-6483/ Published by Elsevier Inc.

acute overexertion. As a result, preventive measures and response to injury is limited to physical therapy (Waters & Rockefeller, 2010) and workload rescheduling (Caruso & Waters, 2008). Currently, assessment of workplace exposure through observation is a common practice in ergonomics (Mathiassen, Liv, & Wahlström, 2013). However, visual assessments are subjective and may fail to accurately quantify physical exposure, integrate multi-faceted traits (Cavuoto & Nussbaum, 2014; Gallagher & Heberger, 2013; Garg & Kapellusch, 2009), and the observation duration and number of workers being observed may be limited (Paquet, Punnett, & Buchholz, 2001). As a result, automatic patient handling and movement activity recognition is important as a first step to reduce risk and prevent caregiver injury.

The development of advanced technology brings the possibility of more complete assessment and monitoring in the nursing workspace. One widely used approach is the computer vision system for monitoring user activity and behavior in nursing rooms (Garg, Owen, & Carlson, 1992). However, computer vision systems require costly installation and maintenance effort. The post-processing of data involves complex video and image algorithms, making the system costly. Furthermore, immobility, occlusion, and varying illuminations raise technical challenges in recognizing objects in video (Chen, Yang, & Wactlar, 2004; Hauptmann et al., 2004). Privacy in video monitoring is also a concern. A wearable sensing system, such as a miniaturized inertial motion unit (IMU), is a promising approach to caregiver monitoring due to the nature of the handling and movement tasks performed. To monitor complex patient handling activities, multiple IMU sensors attached on different body locations are often needed (Zhang, Wong, & Wu 2011; Zhang, Wu, Chen, & Wu, 2009); however, this is a hassle for long-term use and normal patient handling work (Naya, Ohmura, Takayanagi, Noma, & Kogure, 2006).

Compared to daily life activity (DLA) recognition (Alshurafa et al., 2014), patient handling activity (PHA) recognition is a challenging and substantially unexplored topic. PHA is a complex process and usually involves an interactive procedure between healthcare workers and loads (e.g., patients, medical instruments). Moreover, the characterization of PHA includes not only body postures but loads. Safe patient handling activities follow standardized procedures to prevent injury to both patients and caregivers, which are constrained by regulated operation, physical body kinematics, and the temporal constrains posed by the activities being performed. Given these constraints, PHA primitive, also called “action signature,” can be extracted and represented in a low-dimensional manifold space embedded in a high-dimensional input space. Furthermore, these manifolds capture the intrinsic geometry of activities and act as trajectories to characterize different PHAs. Action signatures are usually nonlinear and even twisted, so dimension reduction by linear model such as principal component analysis (PCA) fail to discover the underlying geometric structures.

We propose a novel solution to overcome the aforementioned obstacles in PHA recognition, which comprise a Smart Insole and an action manifold learning (AML) framework. Smart Insole is a novel footwear device that uses an advanced electronic textile (eTextile) fabric sensor technique providing accurate plantar pressure measurement in both ambulatory and static status. Smart Insole looks and feels like a normal insole without any extra cable, antenna, or adhesive equipment. It is also thin, light weight and easy to use, enabling unobtrusive monitoring of human activities.

Action manifold learning is able to project high-dimensional data into a low-dimensional manifold space. By capturing the fundamental signature of action, only the intrinsic primitive structure is preserved in this transform, whereas unrelated motion artifacts and noise are neglected. Therefore, AML not only performs dimension reduction but also suppresses motion artifacts and noise, which efficiently solves the variation problem in both inter-class and intra-class activities. In this proposed framework, raw pressure data are used rather than extracted statistical features, which are more robust because raw data utterly capture the direct pressure variation imposed by the activities.

We conduct a quantitative evaluation in a controlled environment and a real-life longitudinal study for the AML framework. The experimental results show our method succeeds in qualitative profile recognition, PHA recognition, and load estimation with the overall classification accuracy of 98.9%, 86.6%, and 88.3%, respectively.

The organization of the remaining paper is as follows. Section 2 introduces the background and preliminaries, including related work and Smart Insole design. Section 3 elaborates the action manifold learning framework on underfoot pressure maps. Section 4 provides the evaluation results for the proposed AML framework. Section 5 discusses the impact of the number of nearest neighbors, distance metrics, and generalization in the AML framework. Finally, the conclusion and future work are discussed in Section 6.[1]

2. Background and preliminaries

2.1. Related work

2.1.1. Wearable sensors in nursing activity recognition

Wearable sensors have been used to monitor human actions in the nursing environment. Kuwahara et al. (2003) proposed a wearable auto-event-recording system of medical nursing to capture significant events necessary for analyzing medical accidents. Momen and Fernie (2010) used a wireless Sony game controller to identify six nursing activities happening around a patient. They also identified the start and stop times of six simple nursing activities by attaching a single accelerometer sensor to the backs of eight nurses (Momen & Fernie, 2010). Recognizing the importance of awkward postures in the causation of work-related injuries among nurses, recent research efforts have focused on tracking specific postures adopted by nurses (Freitag, Ellegast, Dulon, & Nienhaus,

[1] An early version (Lin, Song, Xu, Cavuoto, & Xu, 2016) was presented at the first IEEE Conference on Connected Health: Applications, Systems and Engineering Technologies (CHASE 2016).

2007). Extent, frequency and duration of specific extreme or awkward body positions were measured in three planes and assessed on the basis of several standards. However, these approaches are obtrusive in use which require sensors attached on the human body. In addition, these approach an important characterization of PHA. Recently, we have proposed a spatio-temporal warping (STW) pattern recognition framework to recognize PHAs (Lin, Xu, Wang, Cavuoto, & Xu, 2016; Lin, Wang, Cavuoto, & Xu), which characterizes the spatio-temporal nature of the plantar pressure distribution.

2.1.2. Manifold learning in activity recognition

Manifold learning has been widely applied in activity recognition by virtue of the capability of capturing the low-dimensional nonlinear manifolds embedded in the high-dimensional input space. Huang et al. (2014) used a dense pressure sensitive bedsheet to produce pressure maps, and the pressure images are processed by locally linear embedding (LLE) and ISOMAP for on bed rehabilitation exercises. Huang et al. (2014) employed manifold learning for Electrocardiograph (ECG) signals dimension reduction and purification. Its applications to human action recognition can be classified into two categories. The first is video-based. For example, Wang, Xu, and Ai (2003) learned the intrinsic object structure for robust visual tracking by using the ISOMAP algorithm. Schwarz, Mateus, Castañeda and Navab (2010) built a low-dimensional prior motion model for simultaneous human full-body pose tracking and activity recognition from time-of-flight (ToF) camera images. Elgammal and Lee (2004) applied LLE to construct human gait manifolds from silhouettes. Blackburn and Ribeiro (2007) recognized human motion by using ISOMAP and dynamic time warping. Li, Chellappa, and Zhou (2009) proposed a discriminative temporal interaction manifold (DTIM) framework as a data-driven strategy to characterize the group motion pattern without employing specific domain knowledge. A maximum a posteriori (MAP) classifier on the manifold is then applied. Jaeggli, Koller-Meier, and Van Gool (2009) presented a method to simultaneously estimate 3D body poses, which are modeled on a low-dimensional manifold, and action categories from monocular video sequences. The approach learns a generative model of the relationship of body pose and image appearance using a sparse kernel regressor. Morariu and Camps (2006) proposed an approach for matching correspondences based on the use of nonlinear manifold learning. The proposed approach does not require similar views, calibration nor geometric assumptions of the 3D environment, and is robust to noise and occlusion. The second is inertial motion unit (IMU) based. For example, Zhang et al. (2011) used LLE to capture the intrinsic structure of IMU data and build nonlinear manifolds for daily life activities. Valtazanos, Arvind, & Ramamoorthy (2013) applied translation manifold to inertial senor data for posture and position tracking.

2.2. Smart insole

In preliminary work, our team has developed the Smart Insole system (Wu et al., 2015; Xu et al., 2012) it enables wide applications such as gait monitoring in daily life (Lin, Wang, Zhuang, Tomita, & Xu, 2016), step counting (Lin et al., 2015), and a timed-up-and-go system for complex ecological environments (Yang, Song, Lin, Langan, & Xu, 2017). In the following, we will briefly introduce the system design and functions in this section.

2.2.1. Hardware design

Smart Insole is a novel wearable device for activity monitoring, which is able to accurately characterize the plantar pressure variation caused by the ongoing activity. It consists of three important subsystems. The first subsystem is the low-cost sensor array including 48 pressure sensors, a 3-axis accelerometer, a 3-axis gyroscope, and a 3-axis magnetometer. The second is the data acquisition and transmission subsystem including a micro control unit (MCU) and a Bluetooth Low Energy (BLE) module. The third is the visualization and graphic user interface (GUI) subsystem.

The low-cost pressure sensor array is based on an advanced conductive eTextile fabric sensor technique (Rofouei, Xu, & Sarrafzadeh, 2010; Xu, Li, Huang, Amini, & Sarrafzadeh, 2011). The eTextile pressure sensor array is used to obtain the high-solution pressure map from feet, which can be efficiently integrated in Smart Insole. The sensor array is coated with a piezoelectric polymer, and the initial resistance between the top-bottom surfaces is large. When extra force is applied on the surface of the polymer, inner fibers will be squeezed together and the resistance becomes smaller. As a result, the output voltage level will be high. Each pressure sensor is 15 mm × 15 mm. With 48 sensors in total, more than 80% of the plantar area is covered.

We designed a printed circuit board (PCB) to integrate the MCU and Bluetooth module, the inertial motion unit (IMU) module, the micro-USB connector, the power switch, and the battery conditioning circuits together. The MCU and Bluetooth are implemented by a single device CC2541 from Texas Instruments. CC2541 also contains an 8-channel, 12-bit, and 0–3.3 volt analogue-to-digital converter (ADC) module, which can provide up to 100 samples per second (Hz). The integrated IMU chip contains a 12-bit accelerometer, a 16-bit gyroscope, and a magnetometer, which is able to capture precise motion information with 9 degrees of freedom motion sensing. The human ergonomic prototype of Smart Insole is shown in Fig. 1 with front view, back view, and lateral view. The Smart Insole is well packaged to avoid the damage from water and moisture.

2.2.2. Smartphone application design

We developed a graphical user interface (GUI) tool on smartphone, as illustrated in Fig. 2. Users can choose on the smartphone GUI tool to collect pressure data, or movement data, or both data when Smart Insole is in use. The pressure distribution map obtained from the eTextile sensor array and insoles orientation can be visualized on the smartphone screen simultaneously. Specifically, the pressure distribution map is obtained when the user puts his weight on the left foot and metatarsal area of the right foot. Fig. 3 shows the plantar pressure distribution maps in a walking event, where center of the pressure is shifting between the toe and heel area in different stages of walking. In addition, vibrations, changes in center of gravity, balance shits, and even hand motions can propagate

Fig. 1. The human ergonomic prototype of Smart Insole: (a) Front view; (b) Back view; (c) Lateral view.

throughout the entire body to influence the pressure distribution of the feet on the ground. For example, the pressure distribution of the feet when a nurse is walking while pushing a wheelchair forward is different from when she/he is lifting one leg of a heavy patient.

3. Action Manifold Learning (AML) framework on underfoot pressure maps

In this section, we will present the AML framework on underfoot pressure maps for patient handling activity (PHA) recognition. The diagram of the overall system design, including Smart Insole and the AML framework for PHA recognition, is shown in Fig. 4. Caregiver activities and recognition results are the input and output of the system.

3.1. Action manifold learning framework

The processing flow of the action manifold learning framework-based PHA recognition is shown in Fig. 5. The AML framework consists of a training stage and testing stage. In the training stage, the high-dimensional pressure data after pre-processing are mapped into a low-dimensional manifold space by constructing the action manifold to find the action signature for each PHA. Patient handling and movement activities (Freitag et al., 2007; Nelson and Baptiste, 2004) are the tasks involving transfer of a load or patient. Safe PHAs follow standardized procedures to prevent risk to the caregivers' lumbar spine and injury to the patient, so the low-dimensional action signature in pressure distribution can be extracted in the manifold space. In the testing stage, the unlabeled actions are mapped into the low-dimensional manifold space by the input-to-manifold projection mapping function and matched to the closest training action manifold.

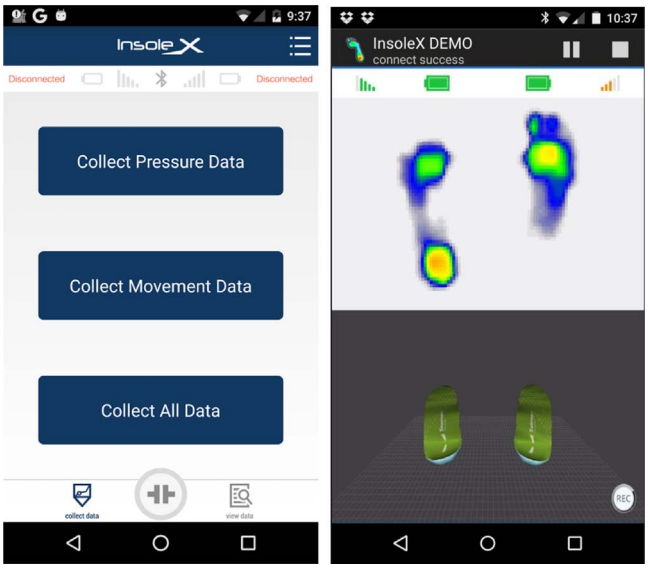

Fig. 2. GUI tool on smartphone for Smart Insole.

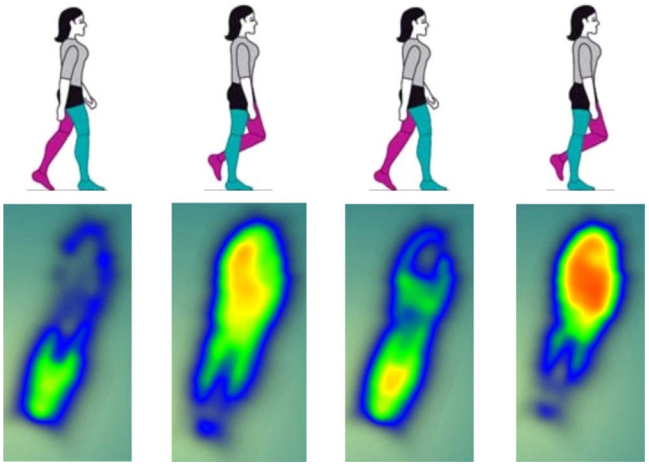

Fig. 3. Plantar pressure distribution maps of right foot in a walking event.

3.2. Pre-processing

The pre-processing of raw pressure maps is required so that the pressure maps can be standardized in such a way to enable successful recognition. First, only the useful primitive action is contained in each set of data samples; unrelated actions or vibrations are eliminated. Second, we obtain the differential of the raw pressure data. The differential of pressure $x_i(t)$ is calculated as:

$$\mathrm{p}_i(t) = \frac{\mathrm{d}x_i(t)}{\mathrm{d}t},\ 1 \le i \le D, \tag{1}$$

where i is the index of pressure sensor, and D is the number of pressure sensor as well as the dimension of the pressure data in input space (in this case $D = 48$). The reason we adopt differential is because it is robust against the spurious signals, different offset of the insoles, and different weights of subjects.

3.3. Action manifold learning

In action manifold learning, we adopt the LLE framework (Saul & Roweis, 2003) to capture the intrinsic low-dimensional structures of the PHA. The reason LLE is a good candidate for action manifold learning is that LLE makes few assumptions about the activities (Saul, Weinberger, Ham, Sha, & Lee, 2006) and runs fast by avoiding the need to solve large dynamic programming problems (Saul & Roweis). After the computation, similar pressure distribution will be clustered within the low dimensional manifold.

Let $\mathbf{P} = \{\mathbf{p}_i \in R^D,\ i = 1,\ldots,N\}$ be the differential of raw pressure data from the PHA signal with sample length of N, where $\mathbf{p}_i$ represents the ith sample of input data and acts as a single point in R^D. Action manifold learning maps D-dimensional $\mathbf{P}$ into d-dimensional manifold space ($d \ll D$). The steps of the LLE procedure are described in the following.

3.3.1. K-nearest neighborhood searching

The first step is to find the K nearest neighbors (kNN) for each point $\mathbf{p}_i$, $i = 1, \ldots, N$ in the input space. In the search process, we use Euclidean distance to measure the similarity between pressure distributions of each sample. The value of K is determined empirically.

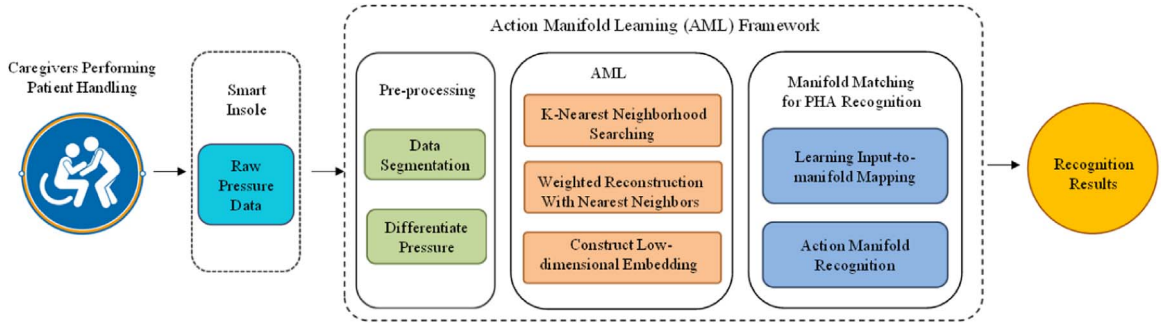

Fig. 4. The diagram of the overall system design, including Smart Insole and the AML framework for PHA recognition.

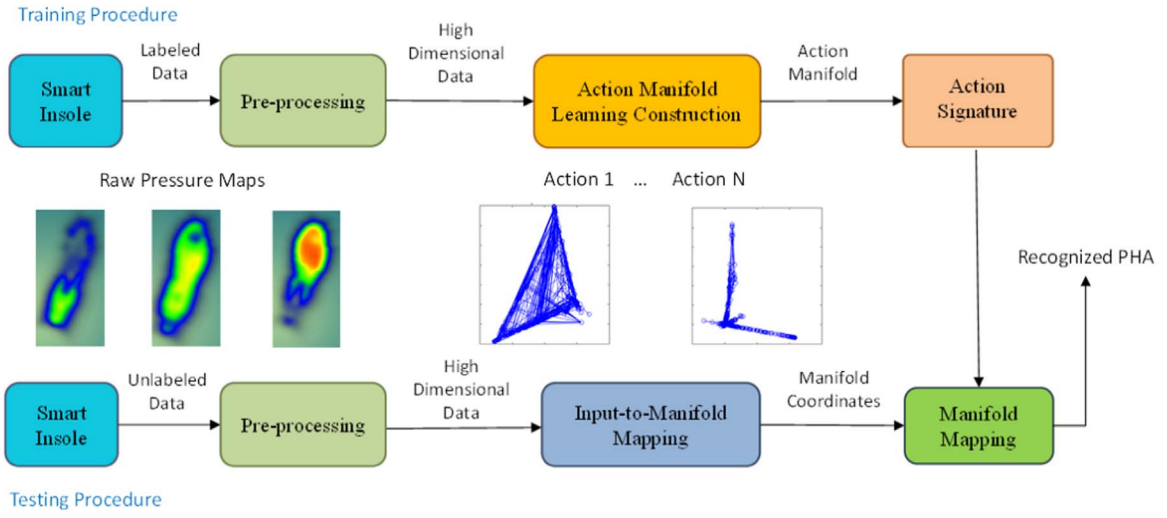

Fig. 5. Processing flow of the action manifold learning-based PHA recognition.

3.3.2. *Weighted reconstruction with nearest neighbors*

The second step is to reconstruct a sample pressure distribution using its nearest neighbors assuming that each point and its nearest neighbors lie on a locally linear patch of the underlying manifold. In practice, an exact reconstruction may not be found, so the reconstruction weights are determined by minimizing the global reconstruction error. The reconstruction error e for a single point can be formulated as:

$$e_i = \left\| \mathbf{p}_i - \sum_{j=1}^{K} w_{ij} \mathbf{p}_{ij} \right\|^2, \tag{2}$$

The global error E can be represented by accumulating N errors together:

$$E = \sum_{i=1}^{N} \left\| \mathbf{p}_i - \sum_{j=1}^{K} w_{ij} \mathbf{p}_{ij} \right\|^2, \tag{3}$$

where w_{ij} denotes the reconstruction weight for the point $\mathbf{p}_i$ and its neighbors $\mathbf{p}_{ij}$. Two constraints are imposed to the cost function (3) to ensure the solution is feasible: (1) $w_{ij} = 0$, if $\mathbf{p}_{ij}$ is not in the nearest neighbors list of $\mathbf{p}_i$; (2) $\sum_{j=1}^{K} w_{ij} = 1$, if $\mathbf{p}_{ij}$ is among $\mathbf{p}_i$'s K nearest neighbors. The solution to Eq. (3) can be found by solving a least square problem (Saul & Roweis, 2003).

3.3.3. *Construct low-dimensional embedding*

The third step is to construct the corresponding embedding in a low-dimensional space. Based on the calculation results from the second step, the intrinsic geometrical structure of each local cluster is characterized by w_{ij}. We assume that the neighborhood relation in high dimensional space should be preserved in low dimensional manifold space. Based on this assumption, the manifold coordinates $\mathbf{y}_i$ can be computed by minimizing the embedding cost function as:

$$\min_{\mathbf{Y}} \Phi(\mathbf{Y}) = \sum_{i=1}^{N} \left\| \mathbf{y}_i - \sum_{j=1}^{N} w_{ij} \mathbf{y}_{ij} \right\|^2, \tag{4}$$

where $\mathbf{y}_i$ and $\mathbf{y}_{ij}$ are the corresponding points of $\mathbf{p}_i$ and $\mathbf{p}_{ij}$ in manifold space, respectively. The cost function can also be written as:

$$\Phi(\mathbf{Y}) = \sum_{i=1}^{N} \sum_{j=1}^{N} \mathbf{M}_{ij} (\mathbf{y}_i \cdot \mathbf{y}_j), \tag{5}$$

involving inner products of the embedding vectors and the $N \times N$ matrix $\mathbf{M}$:

$$\mathbf{M}_{ij} = \delta_{ij} - w_{ij} - w_{ji} + \sum_{k=1}^{K} w_{ki} w_{kj}, \tag{6}$$

where δ_{ij} is 1 if $i=j$, otherwise 0.

All the manifold points $\mathbf{y}_i$ will be computed globally and simultaneously, and no local optima will affect the construction result. Note that the coordinate $\mathbf{y}_i$ can be translated by a constant displacement without affecting the cost $\Phi(\mathbf{Y})$. We require the coordinates to be centered on the origin as:

$$\sum_{i=1}^{N} \mathbf{y}_i = 0, \tag{7}$$

and the embedding points to have unit covariance as:

$$\frac{1}{N} \sum_{i=1}^{N} \mathbf{y}_i \mathbf{y}_i^T = \mathbf{I}, \tag{8}$$

where $\mathbf{I}$ is the $d \times d$ identity matrix. These two constraints make the problem well-posed, thus, the optimal embedding is found by computing the bottom $d + 1$ eigenvectors of the matrix $\mathbf{M}$ and discarding the most bottom eigenvector to get the desired d manifold coordinates (Saul & Roweis).

3.4. Manifold matching for PHA recognition

3.4.1. Learning input-to-manifold mapping

Once the training data have been mapped to its corresponding low dimensional space, we can evaluate the process using new test data against the training data. Since running AML for the entire dataset with training and testing data is computationally expensive, we only execute a portion of the AML algorithm by adopting a non-parametric mapping function (Saul & Roweis, 2003). Given a new test pressure distribution $\hat{\mathbf{p}}$, we wish to find its low-dimensional representation $\hat{\mathbf{y}}$. First, the weights w_j are computed from the K nearest neighbors of $\hat{\mathbf{p}}$ in the training set $\mathbf{p}_i$ by solving the least square problem:

$$\min_{w} \left\| \hat{\mathbf{p}} - \sum_{j=1}^{K} w_j \mathbf{p}_j \right\|, \tag{9}$$

with the constraint $\sum_{j=1}^{K} w_j = 1$. Since the corresponding low-dimensional coordinates of $\mathbf{p}_i$ are known during the training phase, we can reconstruct the embedded coordinates for $\hat{\mathbf{y}}$ using the same weights w_j as:

$$\hat{\mathbf{y}} = \sum_{j=1}^{K} w_j \mathbf{y}_j, \tag{10}$$

where $\mathbf{y}_j$ are the corresponding embedded coordinates of $\mathbf{p}_j$.

3.4.2. Action manifold recognition

The action manifold recognition is performed by comparing the trajectories of manifolds in the low-dimensional space. We observe that the data lengths of each action usually are disparate and different subjects require different times to perform each activity; therefore, an appropriate distance metric that can handle data length misalignment is needed. In this work, we adopt the Hausdorff distance (Wang & Suter, 2006) for a similarity measurement metric. The Hausdorff distance of a point to a manifold is equal to the shortest Euclidean distance to any point in the manifold, that is, the mean value of the minimum, expressed as:

$$s(M_1, M_2) = \frac{1}{T_{M_1}} \sum_{i=1}^{T_{M_1}} \min_{1 \le j \le T_{M_2}} \| M_1(i) - M_2(j) \|, \tag{11}$$

where M_1 and M_2 are two manifolds under comparison, T_{M_1} and T_{M_2} are the number of points in each manifold. Since the Hausdorff distance is directional, we take the summation to ensure the symmetry of the distance metric as:

$$dist(M_1, M_2) = s(M_1, M_2) + s(M_2, M_1). \tag{12}$$

Based on this distance metric, we can measure the similarity between unlabeled activities and known activities, and the testing activity is classified as the activity class which has the most similar manifold with the testing activity. The dimensionality estimation is shown in Fig. 6.

4. Evaluation

4.1. Experimental setup

We ran a series of experiments in a laboratory environment to evaluate the performance of our proposed action manifold learning framework for PHA recognition. The dataset was collected by our Smart Insole from eight subjects including seven male subjects and one female subject. Our team holds an active IRB protocol in the State University of New York at Buffalo (#: 695026-2), which allows for recording motion through wearable sensors while performing patient handling activities. The weights of all participants are from $58 - 85$ kg and heights from 160–185 cm. Each subject performed seven different PHAs including: (a) *bend leg to lift an item from floor level*; (b) *stand while lifting patients leg*; (c) *stand while lifting patient from wheelchair*; (d) *stand while rolling patient*; (e) *walk normally*; (f) *walk while pushing wheelchair forward*; (g) *walk with both hands carrying a chair*. To be specific, in (b), the subject lifted a patient's leg for three seconds then slowly puts down the leg. Likewise, in (d), the subject rolled a patient over and also kept the patient there for three seconds then rolled the patient back to the original position. In (g), the subject first lifted the wheelchair up then walked

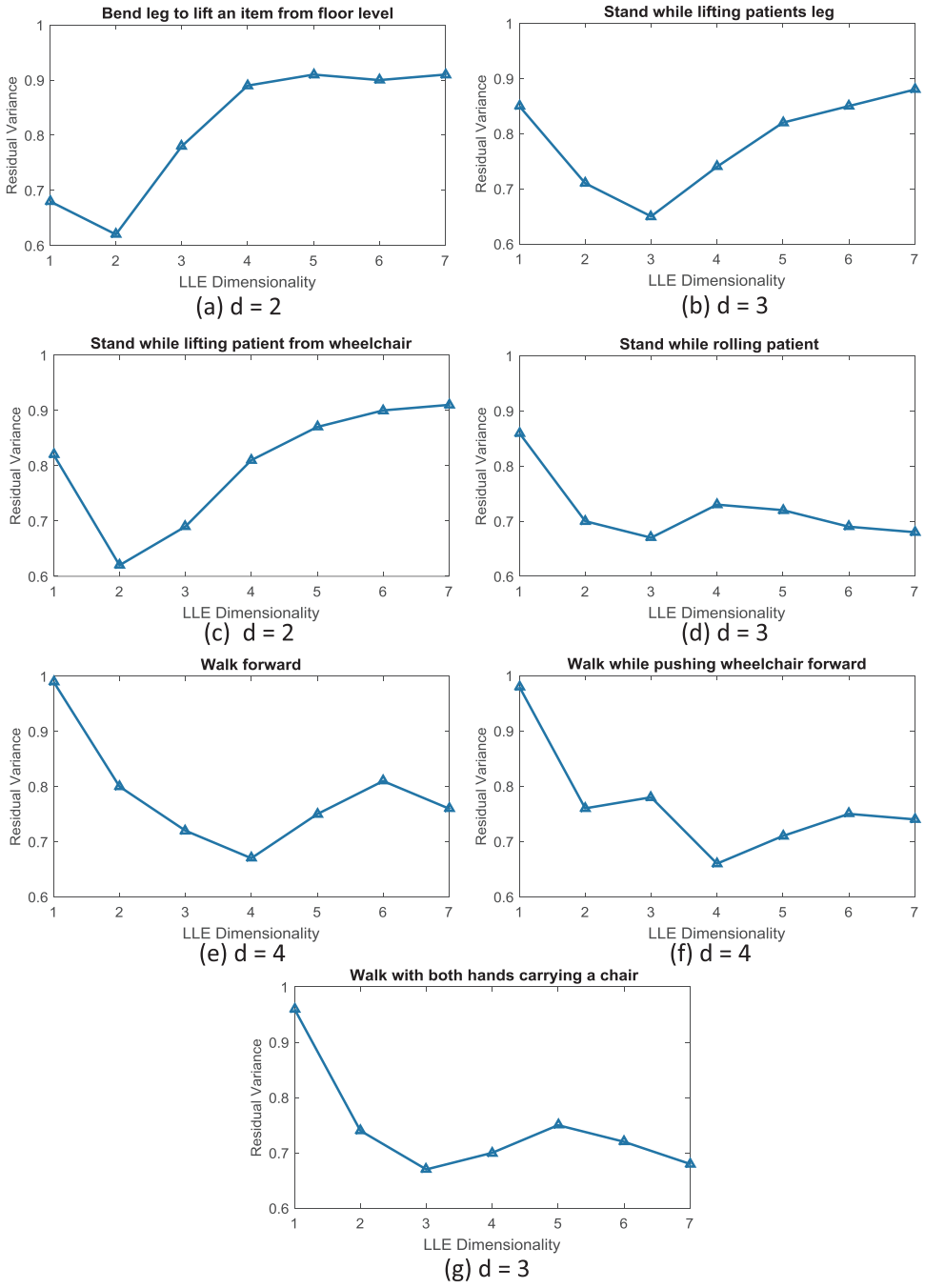

Fig. 6. Intrinsic dimensionality estimation based on residual variance.

forward with two hands carrying the wheelchair. We also performed a *sitting* activity in this evaluation though it is not directly related to patient handling or movement. In addition, sitting is static such that it is infeasible to use the AML framework to extract a consistent trajectory. However, successfully recognizing sitting activity can help to estimate the workload in a nursing environment by knowing how long a caregiver takes a break as sitting. To distinguish sitting from other activities, simply applying a threshold to p_i before AML is enough because sitting is static leading to p_i to be close to 0. For simplicity of description in this paper, we include sitting as one of the PHAs. The real experimental scenes are shown in Fig. 7.

4.2. Action signature extraction

We visualize the 3-D raw pressure data from each PHA in Fig. 8. Since we observed that the data with all 48 channels from Smart

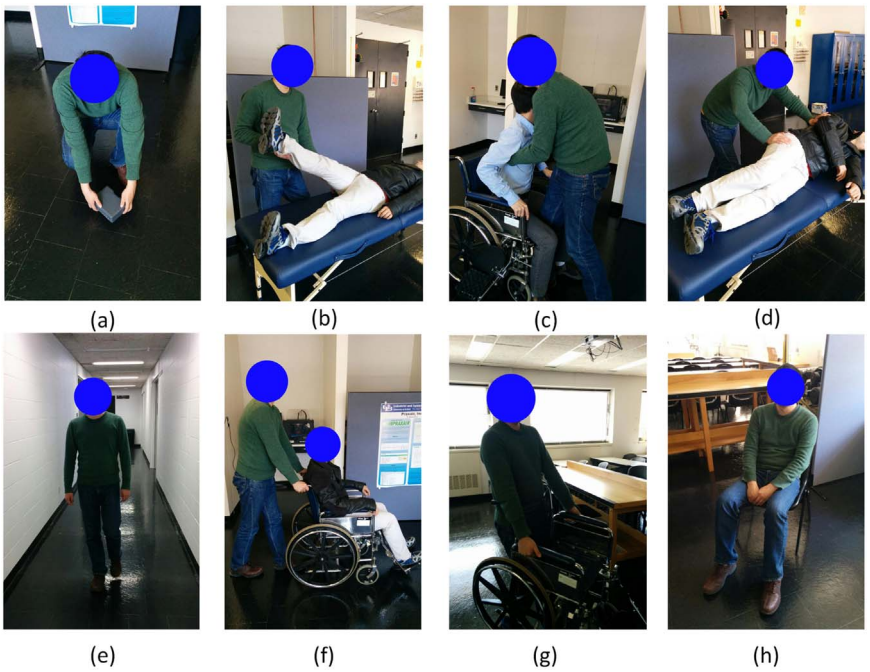

Fig. 7. Eight different PHAs performed in experiments including: (a) Bend leg to lift an item from floor level; (b) Stand while lifting patients leg; (c) Stand while lifting patient from wheelchair; (d) Stand while rolling patient; (e) Walk normally; (f) Walk while pushing wheelchair forward; (g) Walk with both hands carrying a chair; (h) Sitting normally.

Insole in one figure makes the pressure variation pattern too dense to be seen clearly, we pick up six out of 48 pressure points and show their waveforms for a better visualization. In Fig. 8, (a) *bend leg to lift an item from floor level* and (c) *stand while lifting patient from wheelchair* are "single action" based activities. (b) *stand while lifting patient's leg* and (d) *stand while rolling patient* are "action-still-action" based activities, as can be observed from Fig. 8 (b) and (d) that a flat area indicating keeping still exists between two waves indicating actions. (e) *walk normally*, (f) *walk while pushing wheelchair forward*, and (g) *walk with both hands carrying a chair* are all walking related which show either periodic or pseudo-periodic pattern. The corresponding low-dimensional trajectories are shown in Fig. 9. Two "single action" activities (a) and (c) are represented as the crossing lines in two direction. Two "action-still-action" activities (b) and (d) are represented as the crossing lines in three directions. Because the pressure variation in keeping still status is small, the projected trajectory in manifold space as a consequence also has a small deviation, which results in a shorter length compared to the lines in the other two directions. The walking activities in (e), (f), and (g) evolve along a triangle shape in the

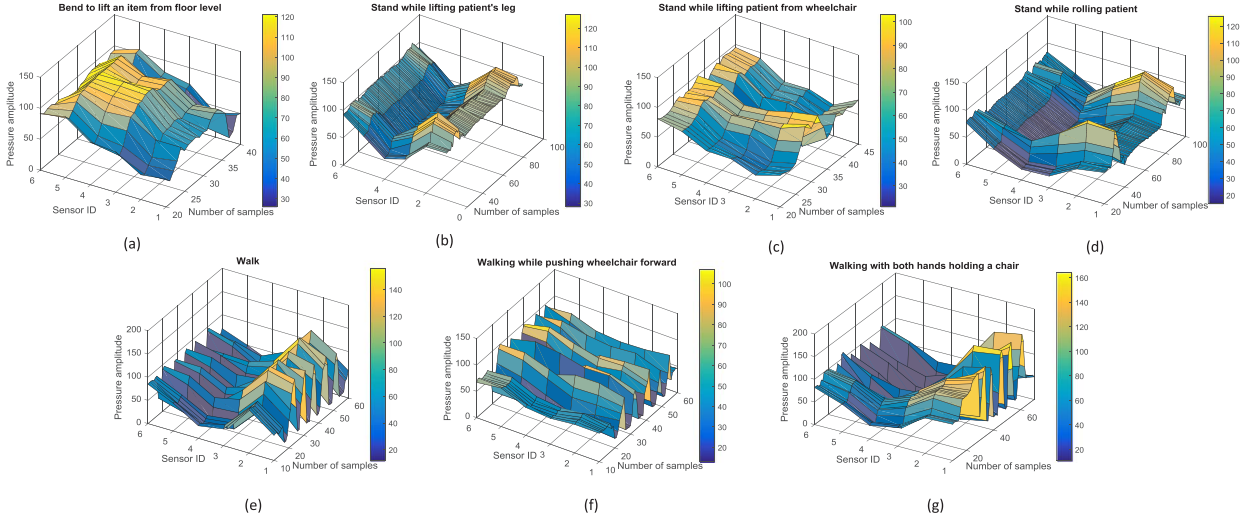

Fig. 8. The 3-D visualization of pressure data from Smart Insole 2.0: (a) Bend leg to lift an item from floor level; (b) Stand while lifting patients leg; (c) Stand while lifting patient from wheelchair; (d) Stand while rolling patient; (e) Walk forward; (f) Walk while pushing wheelchair forward; (g) Walk with both hands carrying a chair.

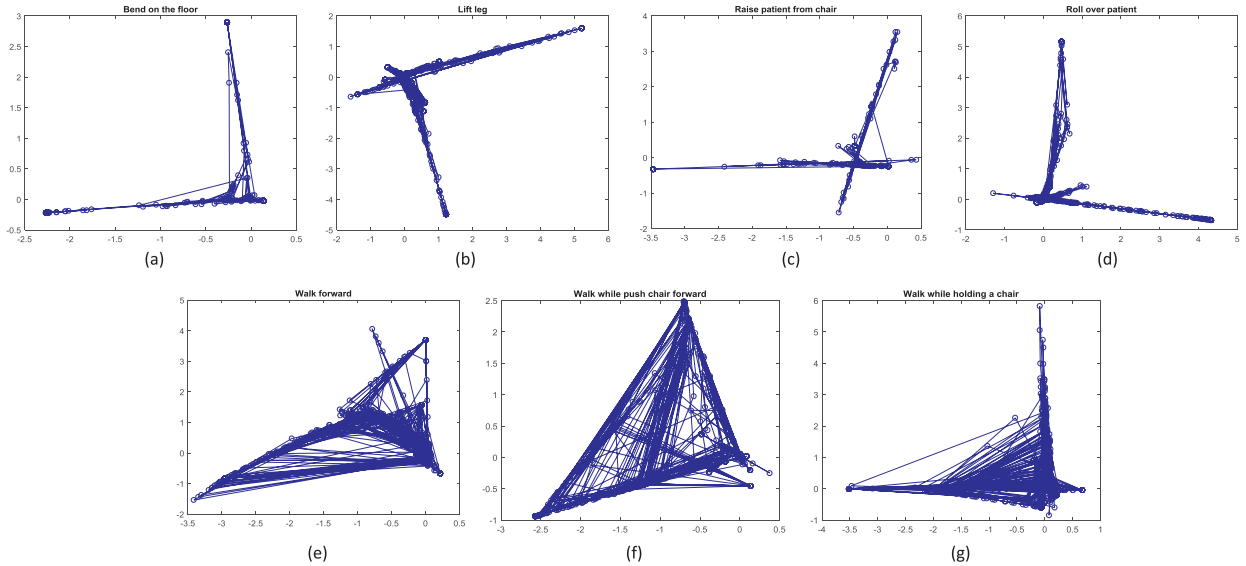

Fig. 9. Visualization of PHA in manifold space: (a) Bend leg to lift an item from floor level; (b) Stand while lifting patients leg; (c) Stand while lifting patient from wheelchair; (d) Stand while rolling patient; (e) Walk forward; (f) Walk while pushing wheelchair forward; (g) Walk with both hands carrying a chair.

manifold space. This is because these three activities are either periodic or pseudo-periodic causing the trajectories of different cycles to overlap with each other. Note that besides walking, (g) also contains a *lifting chair* "single action," which results in the trajectory exhibiting a two crossing lines pattern.

4.3. Intrinsic dimensionality estimation

To accurately reconstruct the pressure distribution of various activities in the manifold space, it is important to know the intrinsic dimensionality of the manifold. In this work, we adopted residual variance (Tenenbaum, De Silva, & Langford, 2000) for the intrinsic dimensionality estimation. The residual variance is defined as

$$Residual\ variance = R^2(D_I, D_M), \tag{13}$$

where D_I, and D_M are the Euclidean distance matrices in the input space and low-dimensional embedding space, respectively. R is the standard linear correlation coefficient of D_I and D_M. We expect a low residual variance between input space and low-dimensional embedding space, and we try to find the intrinsic dimensionality of the manifold d. Fig. 6 illustrates the residual variance change versus manifold's dimension d for different activities. To avoid overfitting, d is found by looking for the "elbow" point at which the residual variance ceases to decrease significantly (Tenenbaum et al., 2000). As seen from Fig. 6, for activities *bend leg to lift an item from floor level* and *Stand while lifting patient from wheelchair*, the estimated intrinsic dimensionality is 2. For activities *stand while lifting patients leg*, *stand while rolling patient*, and *walk with both hands carrying a chair*, the estimated intrinsic dimensionality is 3. For activities *walk forward* and *walk while pushing wheelchair forward*, the estimated intrinsic dimensionality is 4. We noted that comparing with one time interaction with patient or a single activity, walking related activities have most complicated structures since walking is a continuous motion activity. In the following, AML based PHAs are constructed in their own intrinsic dimensionality spaces respectively.

4.4. Quantitative evaluation in a controlled study

For this part, we evaluate the classification performance of our proposed framework by *k*NN. A leave-one-out cross-validation (LOOCV) is adopted to quantify the accuracy. In this quantitative evaluation, each subject is required to perform 10 trials on each activity. Therefore, a total of 640 trials is performed in our experiments.

4.4.1. Accuracy evaluation

The quantitative evaluation performance is measured by classification accuracy. Given the large number of testing inquiries, the framework should offer the correct responses with high probability. The accuracy (ACC) is defined as:

$$ACC(\%) = \frac{TP + TN}{P + N} \times 100\%, \tag{14}$$

where TP represents the true positive, TN represents the true negative, P represents the positive, and N represents the negative. In injury risk estimation, qualitative profile recognition, PHA recognition, and load estimation are three key parameters (Krause, Rugulies, Ragland, & Syme, 2004). PHA recognition is used for estimating injury probability for each PHA. Qualitative profile

Table 1
Confusion table of recognition on three categorized activities.

	Stand (a, b, c, d)	Walk (e, f, g)	Sit (h)	Total	Recall
Stand (a, b, c, d)	315	5	0	320	98.4%
Walk (e, f, g)	2	238	0	240	99.2%
Sit (h)	0	0	80	80	100.0%
Total	317	243	80		
Precision	99.4%	97.9%	100.0%		

recognition and load estimation are used in estimating workload and load in performing PHA, respectively.

4.4.2. Qualitative profile recognition

Qualitative profile recognition is used to estimate the workload in a nursing environment. Research data show that most nurses suffer from chronic occupation-related diseases. Based on the percentages of all-body activities (i.e., walk related), upper-body activities (i.e., standing related), and break (i.e., sitting) in a working period, we can infer the intensity level of the workload and the long-term fatigue level, so that the nurse can pay more attention in PHA to prevent potential injuries. Here, all the aforementioned eight PHAs are categorized into three qualitative profiles as described in Table 1, which facilitates the workload estimation. Both recall and precision achieve more than 97.9% as shown in Table 1, which shows high performance of qualitative profile recognition. Note that the performance from qualitative profile recognition is better than the one with PHA recognition described in the following, which is because several confusing activities actually belong to the same qualitative profile such as *stand* or *walk*. In such case, these PHAs are treated as no difference in terms of qualitative profile. The *ACC* can reach 98.9%.

4.4.3. PHA recognition

The goal of PHA recognition is to accurately classify each PHA defined in Fig. 7. Table 2 shows the confusion table with respect to PHA classification using 48 pressure sensors. We notice the activity *walk with both hands carrying a chair* has the lowest recall rate 80.0%, which is often confused with *walk normally* and *walk while pushing wheelchair forward*. The reason for confusion is that all the three activities are performed in walking status, in which the pressure obtained all show a similar pseudo-periodic nature. Among them, *sit* reaches 100% recall and 100% precision because of the minimal fluctuation it exposed that differentiates it from other activities. In terms of precision, *walk with both hands carrying a chair* also shows the lowest rate of 79.0% because the data from other activities show similarity to the data of *walk with both hands carrying a chair*, which results in misclassification. Overall, the *ACC* can reach 86.6%. This accuracy can be further improved by analyzing IMU data together with pressure data.

4.4.4. Load estimation

The load estimation is to estimate the load imposed on caregivers when they perform certain PHA in order to prevent overexertion. The grouping criterion depends on the specific ongoing activity and how normal people feel when performing it. Note that we classify *bend leg to lift an item from floor level* as *light load* because for that item the subject picked up indicates the specific weight of the object in our experiment. The load level category is summarized in Table 3. Likewise, the confusion table with respect to load levels is shown in Table 4. *Light load* has the lowest recall of 87.1%, and *heavy load* has a similar recall of 87.9%. Since these two load levels both involve forceful exertion, they are easily confused with each other. The ACC can reach 88.3%.

4.5. Evaluation of a longitudinal pilot study

To evaluate the proposed approach in an end-to-end test scenario, we carried out a pilot study in a real nursing room. The subject wearing Smart Insole performed a set of patient handling activities in a continuous manner. The activities include all actions in Fig. 7 in a random sequence. For the sake of repetition, each activity was performed more than once. We also videotaped the entire process

Table 2
Confusion table of recognition on 8 PHAs using AML.

	a	b	c	d	e	f	g	h	Total	Recall (Sensitivity)
a	69	2	7	0	0	0	2	0	80	86.3%
b	2	70	4	4	0	0	0	0	80	87.5%
c	7	2	67	1	0	0	3	0	80	83.8%
d	1	4	2	73	0	0	0	0	80	91.3%
e	0	0	0	0	65	9	6	0	80	81.3%
f	0	0	0	0	8	66	6	0	80	82.5%
g	1	0	1	0	7	7	64	0	80	80.0%
h	0	0	0	0	0	0	0	80	80	100.0%
Total	80	78	81	78	80	82	81	80		
Precision	86.3%	89.7%	82.7%	93.6%	81.3%	80.5%	79.0%	100%		
Specificity	98.0%	98.6%	97.5%	99.1%	97.3%	97.1%	97.0%	100%		

Table 3
Categorization of PHA into load levels.

	Load levels	Activities description
c	Heavy	Stand while rolling patient
d		Stand while lifting patient from wheelchair
g		Walk with both hands carrying a chair
a	Light	Bend leg to lift an item from floor level
b		Stand while lifting patients leg
f		Walk while pushing wheelchair forward
e	No	Sit normally
h		Walk normally

as the label of ground truth. Fig. 10 shows the evaluation results, where the red dash line indicates the ground truth and the blue line indicates the actual classification outcome. We observed that only one out of 24 activities is misclassified, which validates the effectiveness of the proposed AML framework in the real-life setup.

4.6. Comparison with PCA-based dimension reduction

Dimension reduction techniques are usually applied on a large scale dataset to transform data into another domain to either make it more manageable or easy to analyze. PCA is a linear dimension reduction method that has widespread use. Fig. 11 illustrates the visualization trajectories of PCA and AML when performing the *stand while lifting patient from wheelchair* activity. We compare the performance of AML and PCA-based dimension reduction method (Jolliffe, 2002) for PHA recognition in terms of accuracy, as shown in Table 5. PCA has the accuracies of 84.3%, 71.5%, and 72.1% in the qualitative profile recognition, PHA recognition, and load estimation, respectively. Compared with PCA, AML is better suited to identify the underlying topological structure that is nonlinear in the high-dimensional space. Overall, AML outperforms PCA-based dimension reduction.

5. Discussion

5.1. Impact of K in AML

The proper selection of K, the number of nearest neighbors defined in AML, has a big impact on the performance of AML. If K is too small, a continuous manifold may be divided into disjointed sub-manifolds. Actually, the LLE algorithm can only recover embeddings where intrinsic dimensionality is less than K (Saul & Roweis, 2003). In contrast, a large K may violate the assumption of local linearity. Thus, we need to determine the optimal selection of K. We ran an experiment changing K from 2 to 14 steps by 2 to find the optimal K in terms of lowest misclassification error. The performance measured by the misclassification rate is shown in Fig. 12, where the error bars represent the standard deviation. As seen from the figure, the lowest misclassification rate is achieved at $K=6$, and the performance of $K=8$ is slightly worse. We conclude that using 6 nearest neighbors is optimal to construct the activity manifolds.

5.2. Distance metrics

In the AML framework, choosing an appropriate distance metric is a critical step for similarity measurement, such as Euclidean distance (ED) (Joh, Arentz, & Timmermans, 2001), Hausdorff distance (Wang & Suter, 2006), and earth mover's distance (EMD) (Xu et al., 2016; Xu et al., 2015). Among them, Euclidean distance provides 1-to-1 matching; both Hausdorff distance and EMD can

Table 4
Confusion table of recognition on three categorized load levels.

	Heavy (c, d, g)	Light (a, b,f)	No (e, h)	Total	Recall
Heavy (c, d, g)	211	22	7	240	87.9%
Light (a, b,f)	23	209	8	240	87.1%
No (e, h)	6	9	145	160	90.6%
Total	240	240	160		
Precision	87.9%	87.1%	90.6%		

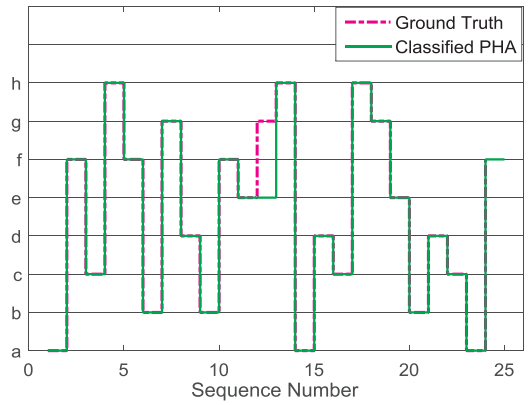

Fig. 10. A set of eight PHAs performed randomly against ground truth. (For interpretation of the references to color in this figure legend, the reader is referred to the web version of this article.)

provide matching under a misalignment situation where Hausdorff distance can solve *m*-to-1 matching (Ding & Xu, 2013) and EMD can solve *m*-to-*n* matching. Compared with ED and EMD, Hausdorff distance is more suitable in our problem and is adopted in our proposed framework. First, ED is unable to handle the misalignment problem caused by the disparate data length of each activity. Second, the computation complexity of EMD is $O(n^3 logn)$ while Hausdorff distance is only $O(n)$, the computation speed of Hausdorff distance is much faster than that of EMD, especially when the dataset is in large scale. Another potential distance metric is Kullback-Leibler divergence, which is a type of probability distance that measures the difference between two probability distributions. It is widely accepted to model ambiguity sets (Hu and Hong, 2012). We will pursue using Kullback-Leibler divergence as the distance metric in our future work.

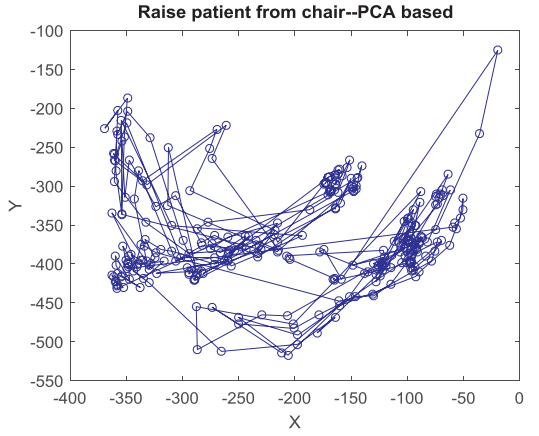

(a) PCA

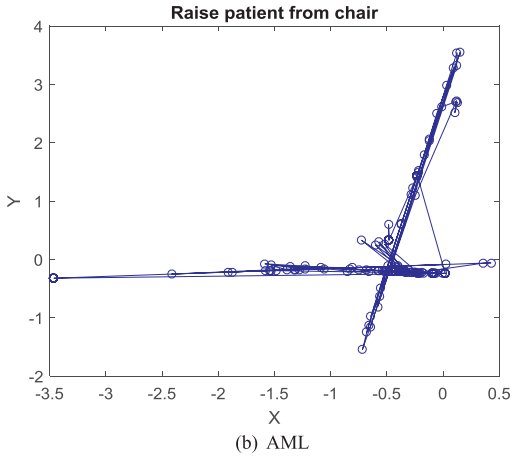

(b) AML

Fig. 11. Visualization of two types of dimension reduction methods.

Table 5
Accuracy comparison between AML and PCA.

	AML	PCA
Qualitative Profile Recognition	98.9%	84.3%
PHA Recognition	86.6%	71.5%
Load Estimation	88.3%	72.1%

5.3. Connection to caregivers' injuries reduction

Our proposed Smart Insole and AML framework can contribute to caregiver injury reduction in multifaceted aspects. The current design of our system mainly focuses on chronic occupational disease prevention. Studies show that most nurses suffer from chronic musculoskeletal disorders due to awkward body postures, overexertion and fatigue caused by working long hours and shiftwork (Waters et al., 2006). Monitoring nurses' work routine and assessing the injury risk possibility is a promising approach to prevent injury. Our system can serve as a cost-effective practical exposure assessment tool for healthcare workers by providing a set of qualitative profiles, patient handling activities, and load recognition, where qualitative profiles with work duration contributes to long-term fatigue; patient handling activities contributes to awkward body posture; and load estimation contributes to overexertion, respectively. Our results can help nurses to monitor their working action in the long-term and support decision making regarding work rescheduling to avoid potentially harmful actions and working fatigue. Our system also holds the potential to recognize acute injuries by incorporating other sensing modalities, such as inertial motion information, with pressure data into the system. Incline degree, instantaneous motion speech, and body orientation can be measured by the inertial motion sensor. A warning signal can be delivered to the nurse to alert the hazardous situation before the nurse gets hurt or feels uncomfortable.

5.4. Generalization of AML

There are tunable parameters in the proposed AML framework (e.g. d, K); the choice of these parameters will make the AML framework achieve good performance in practice. Safe patient handling activities follow standardized procedures to prevent injury, so the intrinsic dimension of PHA primitive d in the low-dimensional manifold space has a small range of variation, which is usually between 2 and 4. The intrinsic dimension can be found by the training process of PHA and used in the classification phase of PHA. From the results presented in Section 5.1, the optimal choice of K is 6.

6. Conclusion and future work

Recognizing patient handling activities is the first step to estimate the physical injury risk for caregivers. We propose a solution comprising Smart Insole and an action manifold learning framework for accurately recognizing PHA. Smart Insole is capable of capturing the plantar pressure change information caused by the PHA. The AML framework can find the intrinsic signature structure by performing nonlinear dimension reduction on raw pressure data from a high-dimensional input space to a low-dimensional manifold space. The experimental results showed that our framework can achieve 86.6% overall accuracy with eight different PHAs. Meanwhile, the qualitative profile and load level can also be classified with accuracies of 98.9% and 88.3%, respectively. Moreover, we also investigated the influence of the number of nearest neighbors (K) to the performance. In AML framework, $K=6$ is the optimal

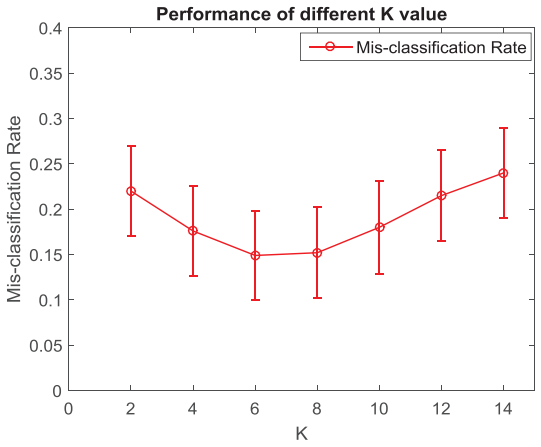

Fig. 12. Performance impact of different K value for action manifold learning.

selection to get the lowest misclassification rate.

Future work involves improvement in three aspects. First, more PHA will be included in the activity set, and the recognition performance using AML framework will be evaluated accordingly. Second, we will improve the PHA recognition accuracy by combining other techniques or other sensing modality. we plan to incorporate IMU data, which are obtained from the IMU sensor embedded in Smart Insole, into the AML framework to better characterize the motion information in another domain. Third, statistical features extracted from the data can also be used to help build the activity manifold model so as to reach a better recognition rate.

Acknowledgment

This work is in part supported by the Pilot Projects Research Training Program of the NY and NJ Education and Research Center, National Institute for Occupational Safety and Health (NIOSH), Grant # T42-OH-008422.

References

Alshurafa, N., Xu, W., Liu, J. J., Huang, M.-C., Mortazavi, B. J., & Sarrafzadeh, M. (2014). Designing a robust activity recognition framework for health and exergaming using wearable sensors. *IEEE Journal of Biomedical and Health Informatics (JBHI)*, *18*(5), 1636–1646.

Blackburn, J., & Ribeiro, E. (2007). Human motion recognition using isomap and dynamic time warping. In *Human motion–understanding, modeling, capture and animation* (p. 285–298). Springer.

Caruso, C. C., & Waters, T. R. (2008). A review of work schedule issues and musculoskeletal disorders with an emphasis on the healthcare sector. *Industrial Health*, *46*(6), 523–534.

Cavuoto, L. A., & Nussbaum, M. A. (2014). Influences of obesity on job demands and worker capacity. *Current Obesity Reports*, *3*(3), 341–347.

Chen, D., Yang, J., & Wactlar, H.D. (2004). Towards automatic analysis of social interaction patterns in a nursing home environment from video. In *Proceedings of the 6th ACM SIGMM international workshop on Multimedia information retrieval, ACM* (p. 283–290).

Ding, H., & Xu, J. (2013). Fptas for minimizing earth mover?S distance under rigid transformations and related problems. In *Proceedings of the 21st annual european symposium on algorithms*.

Elgammal, A., & Lee, C.-S. (2004). Inferring 3d body pose from silhouettes using activity manifold learning. In *Proceedings of the 2004 IEEE computer society conference on computer vision and pattern recognition*, CVPR (p. II-681). vol. 2.

Freitag, S., Ellegast, R., Dulon, M., & Nienhaus, A. (2007). Quantitative measurement of stressful trunk postures in nursing professions. *Annals of Occupational Hygiene*, *51*(4), 385–395.

Gallagher, S., & Heberger, J. R. (2013). Examining the interaction of force and repetition on musculoskeletal disorder risk a systematic literature review. *Human Factors: The Journal of the Human Factors and Ergonomics Society*, *55*(1), 108–124.

Garg, A., & Kapellusch, J. M. (2009). Applications of biomechanics for prevention of work-related musculoskeletal disorders. *Ergonomics*, *52*(1), 36–59.

Garg, A., Owen, B., & Carlson, B. (1992). An ergonomic evaluation of nursing assistants' job in a nursing home. *Ergonomics*, *35*(9), 979–995.

Hauptmann, A. G., Gao, J., Yan, R., Qi, Y., Yang, J., & Wactlar, H. D. (2004). Automated analysis of nursing home observations. *IEEE Pervasive Computing*, *2*, 15–21.

Hu, Z., & Hong, L.J. (2012). *Kullback-leibler divergence constrained distributionally robust optimization*, Available on optimization online.

Huang, A., Xu, W., Li, Z., Xie, L., Sarrafzadeh, M., Li, X., & Cong, J. (2014). System light-loading technology for mhealth: Manifold-learning-based medical data cleansing and clinical trials in we-care project. *IEEE Journal of Biomedical and Health Informatics*, *18*(5), 1581–1589.

Huang, M.-C., Liu, J. J., Xu, W., Alshurafa, N., Zhang, X., & Sarrafzadeh, M. (2014). Using pressure map sequences for recognition of on bed rehabilitation exercises. *IEEE Journal of Biomedical and Health Informatics (JBHI)*, *18*(2), 411–418.

Jaeggli, T., Koller-Meier, E., & Van Gool, L. (2009). Learning generative models for multi-activity body pose estimation. *International Journal of Computer Vision*, *83*(2), 121–134.

Joh, C.-H., Arentze, T., & Timmermans, H. (2001). Pattern recognition in complex activity travel patterns: Comparison of euclidean distance, signal-processing theoretical, and multidimensional sequence alignment methods. *Transportation Research Record: Journal of the Transportation Research Board*, *1752*, 16–22.

Jolliffe, I. (2002). *Principal component analysis*, Wiley Online Library.

Krause, N., Rugulies, R., Ragland, D. R., & Syme, S. L. (2004). Physical workload, ergonomic problems, and incidence of low back injury: A 7.5-year prospective study of san francisco transit operators. *American Journal of Industrial Medicine*, *46*(6), 570–585.

Kuwahara, N., Noma, H., Tetsutani, N., Kogure, K., Hagita, N., & Iseki, H. (2003). Wearable auto-event-recording of medical nursing. In *INTERACT*.

Li, R., Chellappa, R., & Zhou, S.K. (2009). Learning multi-modal densities on discriminative temporal interaction manifold for group activity recognition. In *IEEE conference on computer vision and pattern recognition, CVPR* (p. 2450–2457).

Lin, F., Wang, A., Cavuoto, L., & Xu, W. Towards unobtrusive patient handling activity recognition for injury reduction among at-risk caregivers. *IEEE Journal of Biomedical and Health Informatics, 21* (3).

Lin, F., Wang, A., Song, C., Xu, W., Li, Z., & Li, Q. (2015). A comparative study of smart insole on real-world step count. In *EEE Signal processing in medicine and biology symposium (SPMB)* (p. 1–6). http://dx.doi.org/10.1109/SPMB.2015.7405425.

Lin, F., Xu, X., Wang, A., Cavuoto, L., & Xu, W. (2016). Automated patient handling activity recognition for at-risk caregivers using an unobtrusive wearable sensor. In *IEEE-EMBS international conference on biomedical and health informatics (BHI)* (p. 422–425).

Lin, F., Wang, A., Zhuang, Y., Tomita, M. R., & Xu, W. (2016). Smart insole: a wearable sensor device for unobtrusive gait monitoring in daily life. *IEEE Transactions on Industrial Informatics*, *12*(6), 2281–2291.

Lin, F., Song, C., Xu, X., Cavuoto, L., & Xu, W. (2016). Sensing from the bottom: Smart insole enabled patient handling activity recognition through manifold learning. In *IEEE International conference on connected health: Applications, systems and engineering technologies (CHASE'16)* (p. 254–263). Washington D.C., USA.

Mathiassen, S. E., Liv, P., & Wahlström, J. (2013). Cost-efficient measurement strategies for posture observations based on video recordings. *Applied Ergonomics*, *44*(4), 609–617.

Momen, K., & Fernie, R. (2010). Automatic detection of the onset of nursing activities using accelerometers and adaptive segmentation. *Technology and Health Care: Official Journal of The European Society for Engineering and Medicine*, *19*(5), 319–329.

Momen, K., & Fernie, G. R. (2010). Nursing activity recognition using an inexpensive game controller: An application to infection control. *Technology and Health Care*, *18*(6), 393–408.

Morariu, V.I., & Camps, O.I. (2006). Modeling correspondences for multi-camera tracking using nonlinear manifold learning and target dynamics. In *IEEE Computer society conference on computer vision and pattern recognition* (p. 545–552). Vol.1.

Naya, F., Ohmura, R., Takayanagi, F., Noma, H., & Kogure, K. (2006). Workers' routine activity recognition using body movements and location information. In *Proceedings of the 10th IEEE international symposium on wearable computers, IEEE* (p. 105–108).

Nelson, A., & Baptiste, A. (2004). Evidence-based practices for safe patient handling and movement. *Online Journal of Issues in Nursing*, *9*(3), 4.

Paquet, V. L., Punnett, L., & Buchholz, B. (2001). Validity of fixed-interval observations for postural assessment in construction work. *Applied Ergonomics*, *32*(3), 215–224.

Projected supply. (2002). Demand, and shortages of registered nurses: 2000? 2020, *Technical report.* Health Resources and Services Administration, Bureau of Health Professions.

Public Health Service. (2000). Centers for disease control and prevention worker health chartbook.*Technical report.* US Department of Health and Human Services.
Rofouei, M., Xu, W., & Sarrafzadeh, M. (2010). Computing with uncertainty in a smart textile surface for object recognition. In *IEEE conference on multisensor fusion and integration for intelligent systems (MFI)* (pp. 174–179). Salt Lake City, Utah, USA.
Saul, L.K., & Roweis, S.T. *An introduction to locally linear embedding, unpublished*. Available at: ⟨http://www.cs.toronto.edu/roweis/lle/publications.html⟩.
Saul, L. K., & Roweis, S. T. (2003). Think globally, fit locally: Unsupervised learning of low dimensional manifolds. *The Journal of Machine Learning Research*, *4*, 119–155.
Saul, L. K., Weinberger, K. Q., Ham, J. H., Sha, F., & Lee, D. D. (2006). Spectral methods for dimensionality reduction. *Semisupervised Learning*, 293–308.
Schwarz, L.A., Mateus, D., Castañeda, V., & Navab, N. (2010). Manifold learning for tof-based human body tracking and activity recognition. In *BMVC Citeseer* (pp. 1–11).
Tenenbaum, J. B., De Silva, V., & Langford, J. C. (2000). A global geometric framework for nonlinear dimensionality reduction. *Science*, *290*(5500), 2319–2323.
Texas Instruments. *Cc2541 simplelink bluetooth smart and proprietary wireless mcu* URL ⟨http://www.ti.com/product/cc2541⟩.
Valtazanos, A., Arvind, D., & Ramamoorthy, S. (2013). Using wearable inertial sensors for posture and position tracking in unconstrained environments through learned translation manifolds. In *Proceedings of the 12th international conference on information processing in sensor networks, ACM* (pp. 241–252).
Wang, L., & Suter, D. (2006). Analyzing human movements from silhouettes using manifold learning. In *IEEE international conference on video and signal based surveillance AVSS'06* (pp. 7–7).
Wang, Q., Xu, G., & Ai, H. (2003). Learning object intrinsic structure for robust visual tracking. In *Proceedings of the IEEE computer society conference on computer vision and pattern recognition* (pp. II-227), vol. 2.
Waters, T. R., & Rockefeller, K. (2010). Safe patient handling for rehabilitation professionals. *Rehabilitation Nursing*, *35*(5), 216–222.
Waters, T., Collins, J., Galinsky, T., & Caruso, C. (2006). Niosh research efforts to prevent musculoskeletal disorders in the healthcare industry. *Orthopaedic Nursing*, *25*(6), 380–389.
Work-related musculoskeletal. disorders (wmsds) prevention URL ⟨http://www.cdc.gov/workplacehealthpromotion/evaluation/topics/disorders.html⟩.
Wu, Y., Xu, W., Liu, J. J., Huang, M.-C., Luan, S., & Lee, Y. (2015). An energy-efficient adaptive sensing framework for gait monitoring using smart insole. *IEEE Sensors Journal (SJ)*, *15*(4), 2335–2343.
Xu, W., Li, Z., Huang, M.-C., Amini, N., & Sarrafzadeh, M. (2011). Ecushion: An etextile device for sitting posture monitoring. In *International conference on body sensor networks (BSN)* (pp. 194–199). http://dx.doi.org/10.1109/BSN.2011.24.
Xu, W., Huang, M.-C., Amini, N., Liu, J., He, L., & Sarrafzadeh, M. (2012). Smart insole: A wearable system for gait analysis. In *International conference on pervasive technologies related to assistive environments (PETRA'12)* (pp. 69–72). Crete Island, Greece.
Xu, X., Lin, F., Wang, A., Song, C., Hu, Y., Xu, W. (2015). On-bed sleep posture recognition based on body-earth movers distance. In *IEEE conference on circuits and systems (BioCAS)* (pp. 1–4). Atlanta, GA.
Xu, X., Lin, F., Wang, A., Hu, Y., Huang, M. C., & Xu, W. (2016). Body-earth mover's distance: A matching-based approach for sleep posture recognition. *IEEE Transactions on Biomedical Circuits and Systems*, *10*(5), 1023–1035.
Yang, Z., Song, C., Lin, F., Langan, J., & Xu, W. (2017). Empowering a gait feature-rich timed-up-and-go system for complex ecological environments. In *Proceedings of the 2nd IEEE conference on connected health: Applications, systems and engineering technologies (CHASE 2017),* Washington D.C.
Zhang, Z., Wu, Z., Chen, J., & Wu, J.-K. (2009). Ubiquitous human body motion capture using micro-sensors. In *IEEE International Conference on pervasive computing and communications* , PerCom (pp. 1–5).
Zhang, M., Sawchuk, A., & et al. (2011). Manifold learning and recognition of human activity using body-area sensors. In *Proceedings of the 10th international conference on machine learning and applications and workshops (ICMLA)* (pp. 7–13). Vol. 2.
Zhang, Z., Wong, W. C., & Wu, J. (2011). Wearable sensors for 3d upper limb motion modeling and ubiquitous estimation. *Journal of Control Theory and Applications*, *9*(1), 10–17.